Comparison of new absolute displacement sensors

C. Collette [1,2], S. Janssens [1,2], B. Mokrani [2], L. Fueyo-Roza [1], K. Artoos [2], M. Esposito [2], P. Fernandez-Carmona [2], M. Guinchard [2], R. Leuxe [2]
[1] ULB, Active Structures Laboratory, 50, av. F.D. Roosevelt, 1050, Brussels, Belgium
e-mail: **ccollett@ulb.ac.be**

[2] CERN, Engineering Department, 1211 Geneva 23, Switzerland

Abstract
The measurement of low frequency and small amplitude seismic vibrations with a high accuracy is critical in two scientific disciplines: seismology and structural vibration control. In both fields, there is a constant necessity to develop sensors with a better resolution, robust to temperature variations and magnetic fields, with a low consumption and, of course, at an affordable price. This is particularly valid in frontier science facilities, like future particle colliders and gravitational wave detectors. So far, the vibration sensor industry has not been interested to develop absolute displacement sensors, to measure low frequency and small amplitude vibrations. Such sensors are required in active isolation based on the so-called *sky-hook spring* strategy. In this paper, we show some recent developments and tests of such sensors. Basically, two prototypes are compared. The first one is based on a commercial low cost geophone, which has been modified to measure the displacement. The second one is based on a pendulum. The two sensors are compared on the following aspects: resolution, dynamic range, linearity, spurious high frequency modes, robustness and price

1 Introduction

The last fifty years have witnessed tremendous developments in seismometery [2]. Undoubtedly, the cornerstone of this evolution has been the introduction of the so-called *force balance principle*, which reduces the relative motion between the inertial mass and the support, and allows for a much larger dynamic range than a passive system. Actually, the introduction of this balancing force offers many advantages: (1) to increase the linearity of the sensor (because non-linear effects appear for large displacements), (2) to offer a flat sensitivity to acceleration or velocity at low frequency, which is better for measure seismic signals, and finally (3) to use a high resolution capacitive sensor to measure this relative motion. The principle is now a standard element in seismometers. However, in active control, the amplitudes of interest are relatively small (between 1nm and 10nm), and the quantity of interest is rather the displacement. To some extend, seismometers, seismic accelerometers and geophones can be used for vibration isolation, but the further improvement of active vibration isolation system requires new developments: reduce the size, decrease the noise floor in the frequency range between $0.5\ Hz$ and $100\ Hz$, increase the robustness to environmental disturbances (e.g. magnetic field, radiation, temperature...), and at an affordable price. Compared to commercial products, the needs of inertial sensors for active vibration isolation are illustrated in Fig. 1.

In this paper, two prototypes have been developed to increase the resolution of a commercial geophone. The geophone under test is a GS-11D, Geospace Technologies [4]. Its main properties are summarized in Table 1.

The geophone principle is first reviewed. Then, the new prototypes will be presented and compared.

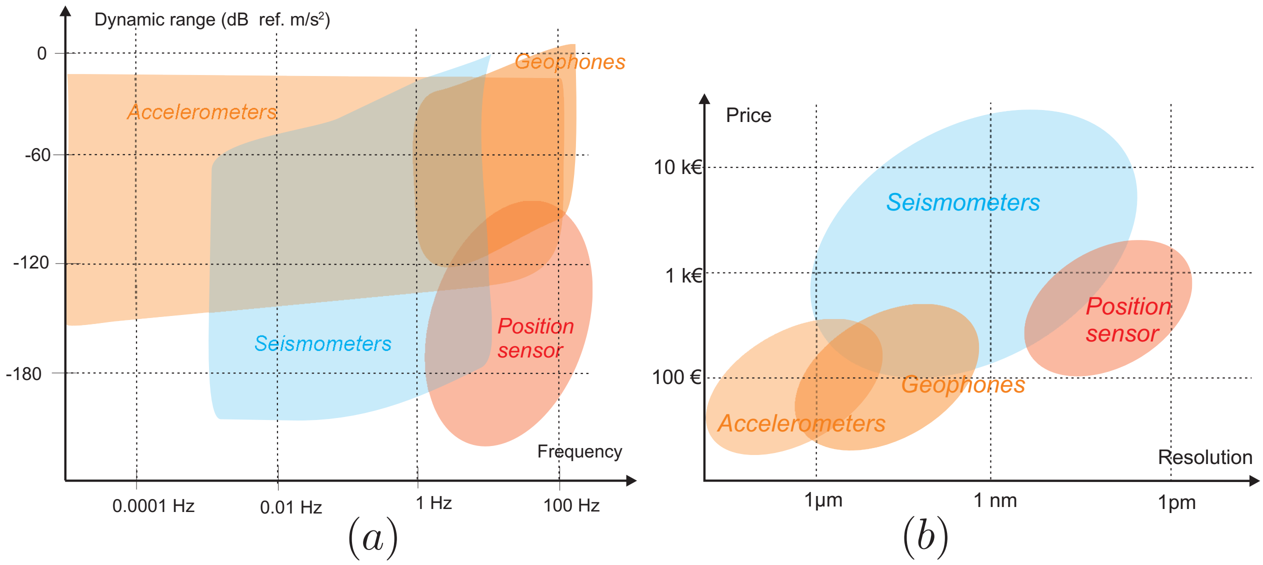

Figure 1: (a) Dynamic range of several types of inertial sensors; (b) Price versus resolution for seveal types of inertial sensors.

Model	GS-11D	Nunmber of turns/coil	3680
Manufacturer	Geospace	Wire diameter	0.06mm
Sensitivity	32 V/(m/s)	Max current I max	90mA
Total weight	0.11 kg	Outer diameter of the coils	27.9mm
Inertial mass	0.018 kg	Stiffness	24 (N/m)
Inner diameter of the coils	25mm	Transducer constant/coil	25N/A
Corner frequency	4.5 Hz	Damping ratio	.50

Table 1: Characteristics of the geophone.

2 Geophone principle

The working principle of the geophone is illustrated in Fig. 2(a). A coil is encircled around a seismic mass m, and loaded by a resistance R. The ground w generates a relative motion between m and the coil. The relative motion creates a current i, and a voltage V_0 across the resistance.

The equations of the system are:

$$m\ddot{x} + c(\dot{x} - \dot{w}) + k(x - w) + Ti = 0 \tag{1}$$

for the mechanical part and

$$L\frac{di}{dt} - T(\dot{x} - \dot{w}) + Ri = 0 \tag{2}$$

for the electrical part, where i is the current, L is the inductance of the coil, and $T =$ is the constant of the coil, expressed in (Tm) or $V/(m/s)$.

Defining $y = x - w$, we get in the Laplace domain

$$ms^2Y + csY + kY + TI = -ms^2W \tag{3}$$

$$LsI - TsY + RI = 0 \tag{4}$$

The output of the sensor is the voltage V_0 across the resistance R, $V_o = RI$. The sensitivity $S(s)$ of the geophone is given by

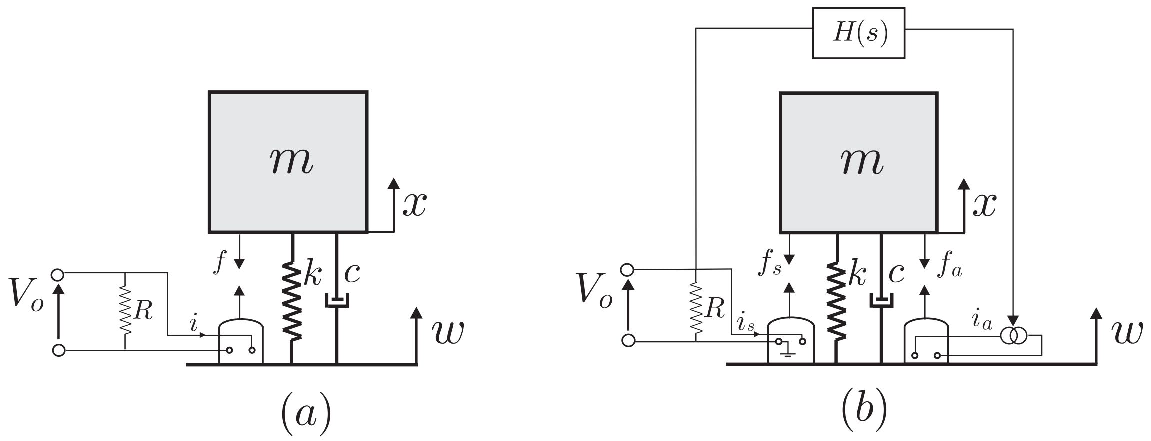

Figure 2: Working principle of (a) a passive geophone and (b) a feedback geophone.

$$\frac{V_o}{sW} = \left(\frac{RT}{Ls+R}\right)\frac{-ms^2}{ms^2+sc+k+\frac{T^2 s}{Ls+R}} \tag{5}$$

In practice, $R \gg sL$ and Equ.(5) is reduced to

$$\frac{V_o}{sW} = \frac{-mTs^2}{ms^2+s(c+\frac{T^2}{R})+k} \tag{6}$$

or equivalently,

$$\frac{V_o}{sW} = \frac{-Ts^2}{s^2+2\xi_0\omega_0 s+\omega_0^2} \tag{7}$$

which is the typical expression of a high pass filter, where $\omega_0 = \sqrt{k/m}$ and $\xi_0 = (c+\frac{T^2}{R})/(2m\omega_0)$. Figure 3 shows the sensitivity curve of the geophone GS11D, in units of (V/m). Typically, geophones can measure the velocity of the support from a few Hertz to a few hundred Hertz. At high frequency, the performances are limited by the higher order modes. At low frequency, the performances are limited by the fundamental resonance of the inertial mass.

In a real sensor, V_0 is polluted by several sources of noise, which are essentially characteristics of the mechanical and electrical components of the sensor (Brownian motion of the seismic mass, Johnson noise, current noise,..) [6]. In this paper, all three contributions are lumped in a quantity N, as shown in Fig. 4(a).

Taking the noise into account, Equ.(7) becomes

$$V_0 = S(s)W(s) + N_s(s) \tag{8}$$

One sees that the smallest detectable quantity is limited by the sensor noise floor N. In practice, N can be measured either combining the output signals of two identical sensors placed side by side, or by tilting the sensor to block the inertial mass [1, 5]. Figure 5 shows the noise floor of the GS11D.

A convenient method to improve the apparent sensitivity of the geophone is to use a stretcher filter, with a double pole at ω_c and a double zero at ω_0, where $\omega_c < \omega_0$ [8, 9]. However, it does not improve the ratio signal/noise of the geophone. In the next section, an alternative method is presented, where the corner frequency of the geophone is actively decreased.

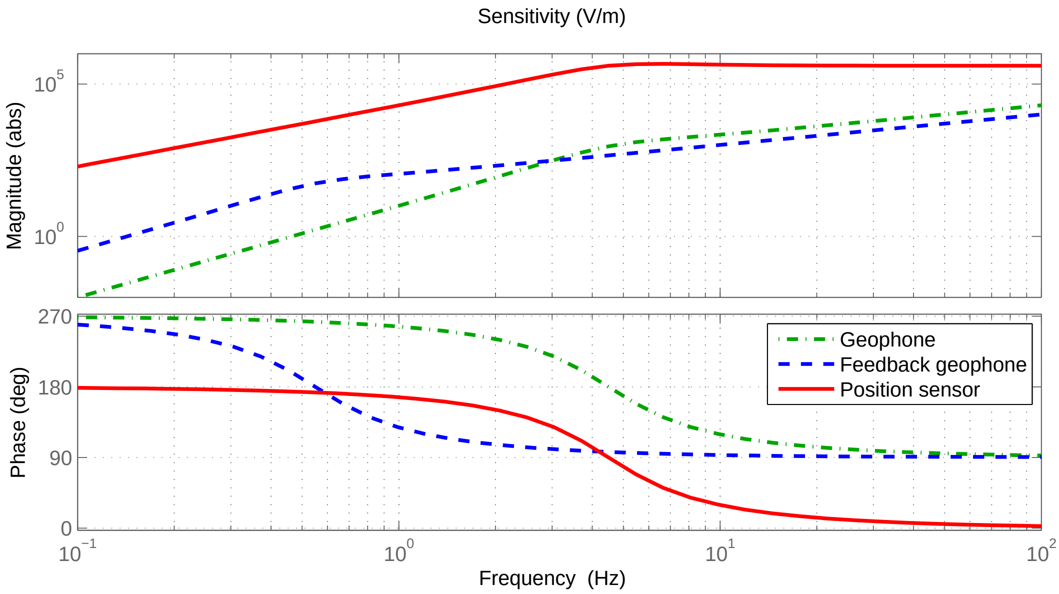

Figure 3: Normalized sensitivity expressed in (V/m) of three sensors: (a) a geophone; (b) a feedback geophone; (c) a position sensor.

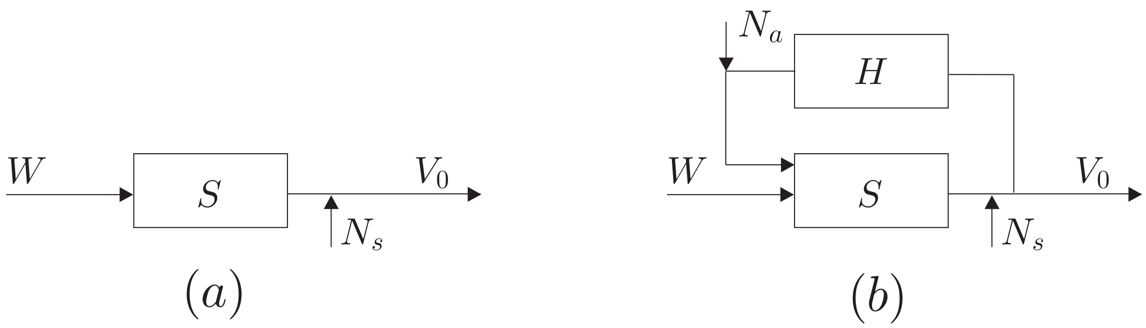

Figure 4: Noise model for (a) a passive sensor and (b) an active sensor.

3 Feedback geophone

The principle of a feedback geophone is shown in Fig. 2(b). The coil is divided in two parts, and (3) becomes

$$ms^2Y + csY + kY + T_aI_a + T_sI_s = -ms^2W \tag{9}$$

where T_s and T_a are the constants of the two parts of the coil. One part is still used as sensor. Using the same assumption that R is large, the output voltage is given by

$$V_o = RI_s \simeq T_s sY \tag{10}$$

where I_s is the current generated by the relative motion between the mass and the ground. Then, V_0 is used to generate a current in the other part of the coil. Taking a Proportional plus Integral plus derivative (PID) controller, we get

$$I_a = H(s)V_0 = (g_p + \frac{g_i}{s} + sg_d)V_0 \tag{11}$$

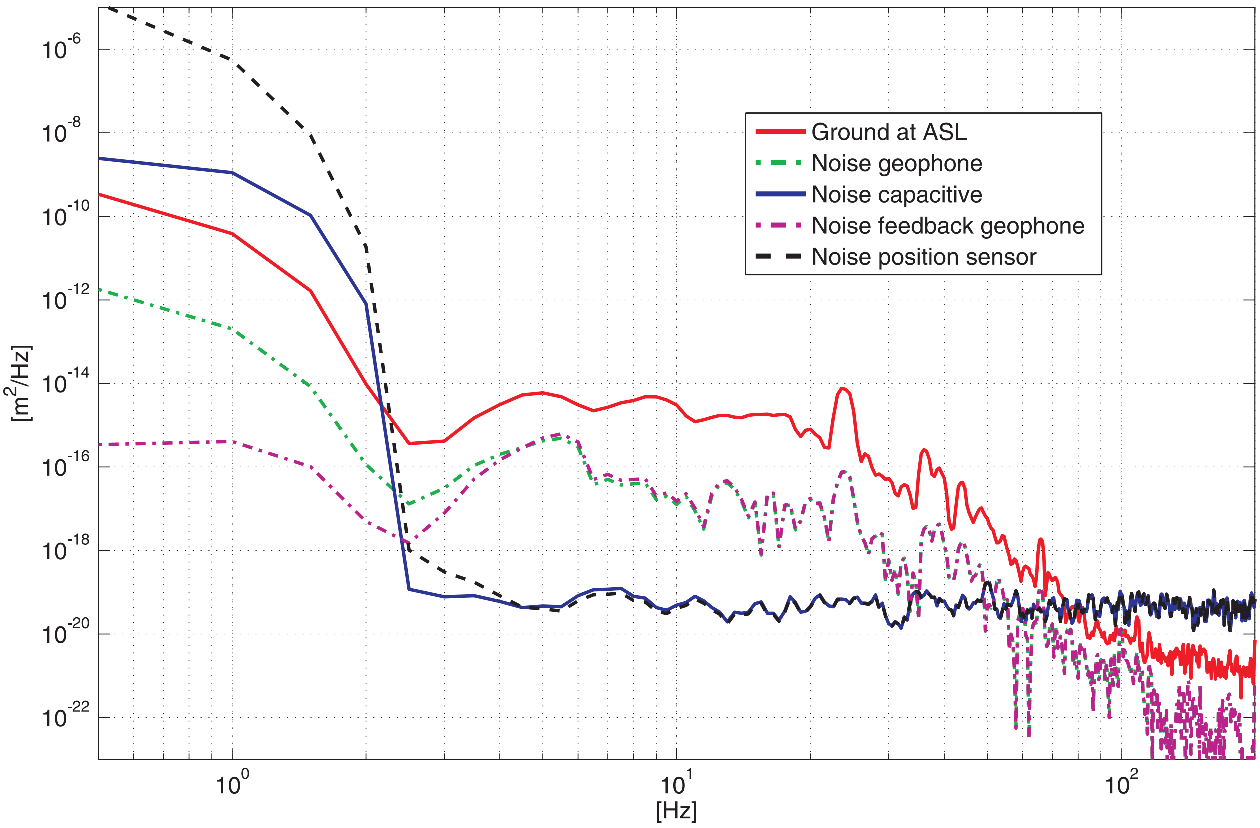

Figure 5: Noise floor of several inertial sensors.

where g_p, g_i and g_d are the gains of the controller. Replacing (10) and (11) in (9) gives the new sensitivity S_{fb}

$$\frac{V_o}{sW} = \frac{-mT_s s^2}{(m + T_a T_s g_d)s^2 + (c + \frac{T_s^2}{R} + T_a T_s g_p)s + k + T_a T_s g_i} \tag{12}$$

which is shown in Fig.3. The corner frequency of the geophone can be actively changed from $\sqrt{\frac{k}{m}}$ to $\sqrt{\frac{k+T_aT_sg_i}{m+T_aT_sg_d}}$ by choosing the values g_i and g_d. The proportional gain g_p is chosen to adjust the damping. In the useful bandwidth, the sensitivity is reduced to

$$\frac{V_o}{sW} = \frac{-mT_s}{m + T_a T_s g_d} \tag{13}$$

and the transfer function between the ground displacement and the relative displacement of the seismic mass is

$$\frac{y}{W} = \frac{-m}{m + T_a T_s g_d} \tag{14}$$

From (13) and (14), one sees that an additional feature of the relative acceleration feedback is that it can modify the sensitivity of the geophone. Choosing a positive value for g_d will force the seismic mass to move with the ground, and reduce the relative displacement of the seismic mass. As a consequence, the sensor will be able to measure much higher levels of vibrations without saturation, which is particularly useful to record strong earthquakes. This is known as the *force balance principle*. On the other hand, choosing a negative value of g_d will increase the sensitivity of the sensor.

This concept has been tested experimentally. The exterior cover of a GS-11D was removed, which decreased the transduction constant, and the coil was separated in two independent parts (Fig. 6(a)).

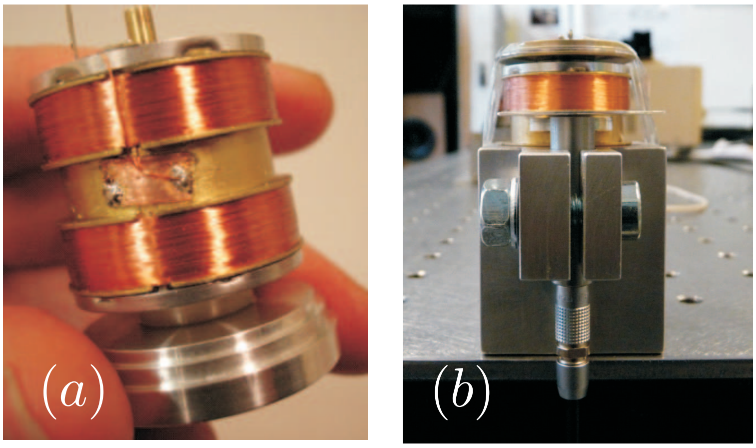

Figure 6: (a) Feedback geophone; (b) Position sensor.

The sensitivity curve in closed loop configuration is also shown in Fig. 3. On the other hand, the increase of the sensitivity is obtained at the cost of the introduction of an additional noise introduced by the feedback operation, as shown in Fig. 4(b). Equations (10) and (11) become

$$V_o = RI_s + N_s = T_s sY + N_s \tag{15}$$

$$I_a = H(s)V_0 + N_a \tag{16}$$

and the output signal of the feedback geophone becomes

$$V_0 = S_{fb} sW + S_s N_s + S_a N_a \tag{17}$$

where S_s and S_a are respectively the sensitivity to the sensor noise and to the actuator noise. Neglecting the actuator noise, the noise curve of the feedback geophone is extrapolated from the noise of the passive geophone, and is shown in Fig. 5. One sees that, compared to the passive geophone, the extension of the sensitivity at low frequencies has reduced the noise curve for frequencies lower than the ω_0.

4 Position sensor

The principle of the an inertial position sensor is based on a direct measurement of the relative displacement between the inertial mass and the support [3]. A thin blade has been fixed on the cylinder which supports the coil. The geophone has been mounted on a new support, on which a capacitive sensor from [7] is also mounted. A picture of the prototype is shown in Fig. 6(b). The sensitivity is shown in Fig. 3, and the noise curve is shown in Fig.5.

5 Comparison and conclusions

The objective of this study is to develop a new inertial sensor, compact, low cost, and with a good resolution at low frequency. Two prototypes of inertial sensors have been presented in this paper. Both of them have been obtained from modifications of a GS-11D. The first one is a feedback geophone, where the sensitivity has been actively increased at low frequencies; the second one is a passive position sensor, where the relative

Sensor	Advantange	Disadvantage
Feedback	- Cheap	- Needs a controller
	- Compact	- Resolution limited
Capacitive	- Good resolution	- Assembly difficult
		- Price
		- Small dynamic range

Table 2: Comparison of two prototypes of inertial sensors.

displacement between the seismic mass and the support is directly measured by a capacitive sensor. The main characteristics of these two prototypes are summarized in Table 2.

In a future work the support of the capacitive sensor will be improved to allow a better alignment. An optical relative sensor is also foreseen as an alternative to the capacitive sensor.

Acknowledgment

The research leading to these results has been partly funded by the European Commission under the FP7 Research Infrastructures project EuCARD, grant agreement No.227579, and by the Brain Back to Brussels program from Brussels Capital Region for the first author.

References

[1] A. Brazilai. *Improving a Geophone to Produce an Affordable, Broadband Seismometer*. PhD thesis, Stanford University, January 2000.

[2] C. Collette, P. Fernandez-Carmona, S. Janssens, K. Artoos, M. Guinchard, C. Hauviller, and A. Preumont. Inertial sensors for low frequency seismic vibration measurement. *Bulletin of the seismological society of America*, To appear in 2012.

[3] P.R. Fraanje, N. Rijnveld, and T.C. Van den Dool. A vibration sensor and a system to isolate vibrations, WO patent No 2009/139628 A1, 2009.

[4] Geospace. `http://www.Geospace.com/`.

[5] L.G. Holcomb. A direct method for calculating instrument noise levels in side-by-side seismometer evaluations. Technical Report 89-214, United States Department of the Interior Geological Survey, 1989.

[6] P.W. Rodgers. Self-noise spectra for 34 common electromagnetic seismometer/preamplifier pairs. *Bulletin of the Seismological society of America*, 1994.

[7] Physik Instrumente (PI) GmbH & Co. PI PISECA 510 Capacitive Nanometrology Position Sensors. `http://www.physikinstrumente.com/`.

[8] L. Zuo. *Element and System Design for Active and Passive Vibration Isolation*. PhD thesis, Massachusetts Institute of Technology, Novemeber 2004.

[9] L. Zuo and S. Nayfeh. An integral sliding control for robust vibration isolation and its implementation. In *Proc. SPIE: Smart Struct. Mater.: Damping Isol.*, volume 5386, page 110, 2004.